LAWRENCE
LIVERMORE
NATIONAL
LABORATORY

LLNL-JRNL-524554

Probing Actinide Electronic Structure through Pu Cluster Calculations

M. V. Ryzhkov, I. R. Schein, A. L. Ivanovskii, A. Mirmelstein, S. W. Yu, J. G. Tobin

January 26, 2012

International Journal of Quantum Chemistry

Disclaimer

Probing Actinide Electronic Structure through Pu Cluster Calculations

M.V. Ryzhkov, I.R. Shein, A.L. Ivanovskii,

Institute of Solid State Chemistry, Ural Division of the Russian Academy of Science, Ekaterinburg, Russia,

A. Mirmelstein,

Department of Experimental Physics, Russian Federal Nuclear Center, E.I. Zababakhin Institute of Technical Physics (VNIITF), Snezhinsk, Russia,

S.-W. Yu and J.G. Tobin,*

Lawrence Livermore National Laboratory, Livermore, CA, USA 94550,
*Corresponding author: Tobin1@LLNL.Gov

Abstract

Calculations of the electronic structure of clusters of plutonium have been performed, within the framework of the Relativistic Discrete-Variational Method (RDV). These theoretical results and those calculated earlier for related systems have been compared to spectroscopic data produced in the experimental investigations of bulk systems, including X-Ray Absorption Spectroscopy (XAS), Photoelectron Spectroscopy (PES) and Bremstrahlung Isochromat Spectroscopy (BIS). Observation of the changes in the Pu electronic structure as a function of size suggests interesting implications for bulk Pu electronic structure.

PAC Numbers: 71.10.-w, 71.20.Gj, 71.27.+a, 71.28.+d

Probing Actinide Electronic Structure through Pu Cluster Calculations

I. Introduction

The development of electronic structure in solid systems as a function of size has long been a subject of great interest and extensive scientific investigation. Experimentally, the transition from nanoscale or mesoscopic to bulk behavior in metal clusters was reported in 1981 by Mason and co-workers. [1] Similarly, the evolution from two-dimensional to three-dimensional band structure in metal overlayers [2] and the manifestation of nanoscale effects in compound semiconductor [3] have also observed. In the area of actinide materials, the progress has been slowed by the limitations imposed by the highly radioactive, chemically toxic and pyrolytic nature of these materials. [4] Havela and Gouder and colleagues performed investigations upon Plutonium (Pu) ultra-thin films deposited in situ by means of a discharge-plasma [5] and Trelenberg and coworkers developed an approach using laser ablation of Uranium (U). [6,7] Gas phase studies of actinides have also been pursued including atoms, [8] molecules [9] and reactions. [10] Recent theoretical studies include UO_2 molecules, [11, 12] solid actinide oxides, [13, 14] and actinide carbide clusters. [15]

Here, we report the result of calculation of the electronic structure of clusters of Pu (Figure 1) and their comparison to bulk spectroscopic results. While the variation of the electronic structure of the Pu clusters as a function of size is in and of itself of great scientific interest, two other considerations raise the value of this study. First, it has become clear that actinide colloids are an important mechanism for the transport on nuclear contaminants in environmental systems [16-18] and it seems likely that predicting the behavior of mesoscopic colloids will require an

understanding of the size dependence of their electronic and physical structures. Second, from a consideration of size dependence of these calculations, important conclusions concerning the bulk electronic structure can be inferred. In particular, it will be seen that the contention that the number of 5f electrons in Pu is near 5 is confirmed. [19]

II. Computational and Experimental Methods

The cluster calculations were performed using the Relativistic Discrete-Variational (RDV) Method. [14, 20, 21] In the bulk limit, a finite fragment of the crystal lattice can be used as a model for the description of some properties of infinite crystal, using the original scheme of "Extended Cluster" boundary conditions. [22] These calculations include a fully relativistic description of the electronic structure basing on the four component Dirac-Slater equation, following the original code of the fully Relativistic Discrete Variational Method (RDV). [23] Underpinning these calculations, there is a geometry optimization of diatomic molecules using scalar relativistic DMol3 and relativistic (inside the spheres) FPLAPW methods. (FPLAPW = fully polarized augmented plane wave.) [24, 25] The results of the cluster calculations will be compared to experimental spectroscopic data from techniques such as X-Ray Absorption Spectroscopy (XAS), Photoelectron Spectroscopy (PES) and Inverse Photoelectron Spectroscopy (IPES), also known as Bremstrahlung Isochromat Spectroscopy (BIS) at high energies, from the corresponding bulk samples. [4, 19, 26-28] The synchrotron-radiation-based PES and XAS measurements were performed mainly at the Advanced Light Source, as described elsewhere. [4, 19, 26, 28] The X-ray PES (XPS) and IPES/BIS

measurements were carried out at LLNL using a spectrometer dedicated to radioactive samples [29], as discussed in References 27 and 28.

III. Confirmation of Comparison Method using U and Pu Oxides

Before going on to a consideration of the new Pu cluster results, it is of some utility to briefly consider the comparison of earlier cluster calculations using this approach [14] and spectroscopic data from the corresponding bulk systems, [4, 19, 26, 28, 29] shown in Figures 2 and 3. The Uranium Dioxide case is illustrated in Figure 2. The lower half of the figure includes partial and total density of states calculations for the 7p, 7s, 6d and 5f states of Uranium and the 2p states of Oxygen, from the central part of a $U_{63}O_{216}$ cluster. The only manipulation of the experimental spectra was to align the centroid of the leading edge of each spectrum with the energy zero in the calculations. In other words, the centroid of the leading edge is treated as if it were a Fermi Edge. The level of agreement here is very strong. On the Occupied Density of States (ODOS) side, the experimental U5f and O2p peaks, from X-ray Photoelectron Spectroscopy (XPS), match quite closely with their theoretical ODOS counterparts. On the Unoccupied Density of States (UDOS) side, both the X-ray Absorption Spectroscopy (XAS) and Bremstrahlung Isochromat Spectroscopy (BIS) features match up with the appropriate theoretical O2p, U5f, and U6d counterparts. The Plutonium Dioxide comparison is plotted in Figure 3. Here, the theoretical Occupied Density of States (ODOS) is shown for the $6p_{1/2}$, $6p_{3/2}$, 5f, 6d, 7s and 7p of Pu and the 2p and 2s of Oxygen, for the central part of the $Pu_{63}O_{216}$ cluster. The experimental synchrotron radiation photoelectron spectrum is from a slightly oxidized Pu sample, taken at the Cooper Minimum using a photon energy of

225 eV. By working at the Cooper Minimum, the non-Pu5f features are emphasized. Again, the only manipulation is to align the Fermi Edge of the PES spectrum with the energy zero of the calculations. The result is again very good agreement, including the placement of the $Pu6p_{1/2}$, O2s, $Pu6p_{3/2}$, O2p and Pu5f peaks. Having confirmed the validity of this approach, the discussion will again return to the issue of Pu clusters.

IV. Pu Clusters

IVa. Electronic structure calculations for Pu_{19}

Underlying the Pu cluster simulations is the calculation of the electronic structure of a Pu_2 dimer with the bond length 3.28 Å, corresponding to the interatomic distances in δ-Pu. [20,30] In the crystal lattice of fcc δ-Pu, each metal site has twelve nearest neighbors and it is evident that the structure of chemical bonding for such a coordination differs essentially from that for a simple linear molecule. As a first step of investigation of chemical bonding and the role of 5f electrons in δ-Pu, we consider the simple cluster model of this crystal consisting of only nineteen plutonium atoms. The structure of this cluster is illustrated in Figure 1. The electronic structure of the Pu_{19} cluster was calculated using the RDV method with local exchange-correlation potential [31]. For the modeling of boundary conditions we used an "extended cluster" scheme described in details in Refs. [32,33]. In this model, the crystal fragment under study consists of two parts: the internal main part (or the "core" of the cluster) and the outer part (or the "shell"). The outer part usually includes the atoms from 1 to 5 coordination spheres surrounding the "core". During the self-consistency procedure, the electron

densities and the potential of the atoms in the "shell" are replaced by the corresponding values obtained for the crystallographically equivalent centers of the cluster "core." To introduce the long-range component of the surrounding-crystal potential, the extended cluster is embedded into a pseudopotential formed by the outer crystal lattice, which includes a few thousands of centers. Coulomb and exchange-correlation potentials of these pseudo-centers are also substituted by the corresponding values obtained for the equivalent atoms in the internal part of the cluster [34].

Since in the present calculations we are interested in the interaction of the central atom with its nearest neighbors, the "core" of Pu_{19} cluster includes only one atom in the center of cluster (labeled below as Pu1). Twelve plutonium sites of the next coordination sphere (Pu2) and six next nearest neighbors (Pu3) form the "shell" and, during self-consistency, their electron densities and potentials were kept equivalent to those of Pu1. The extended bases of the 4-component numerical atomic orbitals also included $7p_{1/2}$ and $7p_{3/2}$ functions. To ensure the convergence of valence molecular orbital (MO) energies within 0.1 eV, numerical Diophantine integration in matrix elements calculations was carried out for a set of 102000 points.

The total and partial densities of states obtained for the central Pu1 atom in Pu_{19} cluster are shown in Figure 4. Since the partial DOS for $7p_{1/2}$ and $7p_{3/2}$; $6d_{3/2}$ and $6d_{5/2}$; $5f_{5/2}$ and $5f_{7/2}$ are close to each other, the sums of DOS for these MOs are presented in the figure. A consideration of the DOS in Figure 4 shows that these are not discrete molecular levels [20, 30] but rather real energy bands of various widths.

For example, 76 MO levels of $6p_{3/2}$ type in Pu_{19} form an energy band with a width of about 2.5 eV. However, the spin-orbital splitting of $6p_{1/2}$ and $6p_{3/2}$ states is about 10 eV: for Pu_{19} this value was obtained for the centers of gravity of Pu$6p_{1/2}$ and $6p_{3/2}$ bands. Another important feature concerns the 6d band. As distinct from a molecule [20,30], many states of this type turn out to be occupied in the Pu_{19} cluster. (Figure 4) The electronic structure transformation, when going from a molecule to the cluster, is accompanied by a considerable (nearly three times) increase of the width of vacant electronic states. Particularly, the highest 7p levels have the energy close to 14 eV. There is no energy gap in the Pu_{19} cluster, i.e. the energy difference of Highest Occupied Molecular Orbital (HOMO) and Lowest Unoccupied Molecular Orbital (LUMO) is less than 0.01 eV. The HOMO in Pu_{19} contains 52% of 5f Atomic Orbitals (AOs) of the Pu2 sites and 13% of the Pu3 5f states with admixtures of Pu2 6d (19%) and Pu3 6d (8%). There are no noticeable contributions to HOMO from any states of central Pu1 atom. On the contrary, the LUMO contains 17% of Pu1 5f AOs, though the main contributions are also belong to Pu2 5f (32%) and Pu3 5f (23%) states.

IVb. Electronic structure of Pu_{79} cluster with fcc crystal-lattice boundary conditions

The next step is to investigate the influence of crystal boundaries on the electron density redistribution shall be the consideration of the greater size Pu_{79} clusters. The previously studied simplest cluster model of δ-Pu contained only nineteen atoms, i.e. the central atom and the nearest and next nearest neighbors (Figure 1). Now, this Pu19 cluster can serve as a “core” of the new fragment

containing 79 atoms, i.e. the Pu_{79} cluster (Figure 1). However, in this case, there are no any restrictions with respect to the electronic characteristic of Pu2 and Pu3 centers during calculations. All three types of atoms in the "core" are considered simply as nonequivalent atoms in a molecule. The "shell" around the cluster "core" is formed by the atoms of the three next coordination spheres (24Pu4, 12Pu5, and 24Pu6) providing the complete set of nearest neighbors for the atoms of a "core". During self-consistency, the electron densities and potentials of Pu4, Pu5, and Pu6 were kept equivalent to those of Pu1. To ensure the convergence of valence MO energies within 0.1 eV, numerical Diophantine integration in matrix elements calculations was carried out for 354000 sample points.

The total and partial densities of states (DOS) obtained for the central Pu1 atoms in the Pu_{19} and Pu_{79} clusters are shown in Figures 4 and 5, respectively. Since the partial DOS for $7p_{1/2}$ and $7p_{3/2}$; $6d_{3/2}$ and $6d_{5/2}$; $5f_{5/2}$ and $5f_{7/2}$ are close to each other, the sums of the DOS for these MOs are presented in the figure. The comparison of results obtained for Pu_{19} and Pu_{79} shows that the positions and widths of the internal $6p_{1/2}$ and $6p_{3/2}$ bands are close in both cases, but the shapes of the bands are noticeably different. The line shape of external 6d states also transforms significantly. Also, the left edge of this band shifts towards the lower energy (towards the higher binding energy), so that the energy difference between these edges in Pu_{79} and Pu_{19} clusters is 0.8 eV. At the same time, the upper edges of 6d bands in both cases lie at the same energy, ~ 11 eV above the Fermi level (usually taken as zero of the energy scale). On the other hand, the positions and widths of the 5f bands are close in both clusters. The only difference is found for

their line shape. In both clusters, the occupied part of valence band is formed by the hybridized 5f – 6d orbitals, but the states at the bottom of this band are mainly of 6d character. The most pronounced difference is revealed for the delocalized 7s and 7p bands. The increase of cluster size leads to the increase of 7p AO contributions to the molecular states within the energy range between 0 and 5 eV above the Fermi level and to the considerable shift of the upper edge of 7s (from 13.5 eV in Pu_{19} to 17 eV in Pu_{79}) and 7p (from 14 eV in Pu_{19} to 19 eV in Pu_{79}) bands.

Similarly to the case of Pu_{19} cluster, there is no energy gap in the Pu_{79} cluster, i.e. the energy difference between HOMO (the highest occupied molecular orbital) and LUMO (the lowest unoccupied molecular orbital) is less than 0.01 eV. The HOMO in Pu_{79} contains only 3% of 5f AOs of the Pu1 site, 5% of 5f AOs of the Pu2, and 4% of the Pu3 5f states with admixtures of 3% of 6d AOs of these atoms, i.e. the main contributions to the HOMO comes from the atoms of cluster "shell", namely, the 5f Pu4 (29%), 5f Pu5 (7%), and 5f Pu6 (32%). In the small Pu_{19} cluster there are no contributions to the HOMO from any states of central Pu1 atom. On the contrary, the LUMO of the Pu_{19} cluster contains 17% of the Pu1 5f AOs while in the LUMO of the Pu_{79} cluster, there are no contributions from the wave functions of the central atom. The main contributions to the LUMO of the Pu_{79} cluster, as well as to the HOMO, belong to the Pu2 5f (19%) and Pu6 5f (35%) states.

Since the iteration process for the Pu_{79} cluster involves two additional types of atoms, one can estimate the sensitivity of the different cluster regions (types of atom) to the cluster boundary. By considering Figures 5 and 6, we can compare the calculated DOS for the Pu1 and the Pu2 sites in the Pu_{79} cluster. As can be seen, the

positions and widths of most of the bands are close for both atom types: even the line shapes of 5f states are similar. Considerable transformation of the DOS is observed for 7p orbitals. Apart from the pronounced qualitative difference in the 7p DOS intensity within the energy range between 0 and 10 eV, the DOS for the Pu1 contains noticeable negative contributions at the energies near 13 eV. This negative DOS results from the overlap of 7p wave functions of the central Pu1 with orbitals of the quite distant atoms in the crystal lattice. Such a difference in the DOS of Pu1 and Pu2 is quite reasonable since the actinide 7p orbitals are extremely delocalized and overlap with the electron density of atoms belonging to distant coordination spheres. The latter feature of these states makes the inclusion of 7p wave functions to the basis quite questionable. On one hand, the extended basis set increases the variation freedom. On the other hand, calculations can give a negative value of occupation of this orbital, or the 7p occupation can accumulate the electron density belonging to other atoms. For this reason, the present stage of this investigation, as in Section IVa above for the Pu_{19} cluster, includes two types of calculations: those with and without 7p basis functions.

IVc Comparison to Experimental Spectra

The data in Figure 7 is a series of synchrotron radiation spectra taken using a slightly oxidized Pu sample. This Pu sample was alpha with a delta-like reconstruction on the surface. [4, 19] By varying the photon energy, it is possible to emphasize or de-emphasize certain features. For example, on resonance at hv = 125 eV, the Pu5f states near the Fermi energy are enhanced. At the anti-resonance with hv = 100 eV, the Pu5f are suppressed and the remnant at the Fermi Edge, including

the Pu6d, is revealed. The spectrum at 180 eV is off-resonance, providing a picture with intensities that reflect the more usual cross sections. [35] Utilizing the Cooper Minimum in the Pu 5f cross section at hv = 225eV is another way to reduce the Pu5f intensity and enhance the other features. If these spectra are compared to the calculated Occupied Density of States (ODOS, energies below zero) in Figures 4, 5 and 6, it is clear that there is good agreement for the Pu5f, Pu6d, $Pu6p_{1/2}$ and $Pu6p_{3/2}$ manifolds.

IVd State Occupations

It is useful to consider the question of state occupation as a function of size. Table 1 contains a summary of the state occupations for the Pu_{19} and Pu_{79} clusters, including a breakdown by sites. One aspect of these calculations is that there can be negative occupations reflecting transfers of electronic density to other atoms. This happens particularly with the most dispersive states, those of 7p character. The impact of the effect is strengthened, by a type of electro-negativity: these sites are not all equivalent and charge transfer can occur. However, it is possible to calculate a weighted average of the occupations, multiplying each configuration's population by the number of atoms of that site type, summing over all sites types and then dividing by the total number of atoms in the cluster. The result is the average configuration, which has the reassuring result that the total number of electrons in the valence range is eight. Of course, eight is the number of electrons that should be on Pu, outside of the Radon-like atomic-center with 86 electrons.

Now consider the occupation of the 5f states as a function of size. For comparison, Table 2 shows the populations for two other Pu structures, a Pu dimer

and a Pu atom. The 5f population decreases monotonically from the atom ($n_{5f} = 6$) to the dimer ($n_{5f} = 5.85$) to the Pu_{19} cluster ($n_{5f} = 5.66$) to the Pu_{79} cluster ($n_{5f} = 5.33$). It is possible to plot this relationship as a function of size. However, this raises the issue of the proper abscissa. These are three-dimensional systems, so the convergence to bulk behavior will occur cubically. Thus, it is proposed here that the correct abscissa should be the cube root of the number of atoms in the system. The results of this operation are shown in Figure 8. It is significant that the four points, for the atom, dimer and two clusters, produce a linear relationship. By fitting a least squares line to these four points, it is possible to extrapolate to other possible cluster sizes. However, it should be noted that in real systems, one would not expect this linear relationship to extend indefinitely. More likely, one would observe an asymptotic approach to limiting behavior, for example, the onset of bulk characteristics.

Nevertheless, it is useful to consider what might be the effect of extrapolating to larger cluster size. From the work of MG Mason et al [1] on metal clusters, minimum cluster sizes of hundreds of atoms are required for the convergence from mesoscopic to bulk behavior. This would imply the cube root of the number of atoms (N) be on the scale of 5 (125 atoms), 6 (216 atoms) or 7 (343 atoms). This picture is supported by the work on metal overlayers, where the development in metal ultra-thin films from two-dimensionality to three-dimensionality occurs around 5 atomic layers. [2] However, it is reasonable to expect that convergence in two-dimensional overlayers will occur at a slightly lower thickness than the convergence in clusters, where all three dimensionalities are evolving in parallel.

Thus, the 5-atom layer estimate should be viewed as a lower limit. Returning to the linear extrapolation for $^3\sqrt{N}$ = 5, 6 and 7, the following results are obtained: for $^3\sqrt{N}$ = 5, n_{5f} = 5.2; for $^3\sqrt{N}$ = 6, n_{5f} = 5.0; for $^3\sqrt{N}$ = 7, n_{5f} = 4.85. This is in quite good agreement with spectroscopically derived estimates that $n_{5f} \approx 5$, which are based upon the data shown in Figure 9. [19] These spectroscopic based arguments are somewhat involved and require looking across the actinides series, but in essence reduce to two key points: the absence of a pre-peak in the Pu 5d XAS and the non-statistical branching ratio in the PU 4d XAS, as shown in Figure 9.

V. Summary and Conclusions

Calculations of the electronic structure of Pu clusters have been performed. Spectroscopic results from bulk samples have been compared to the Density of States results for the Pu clusters and earlier work on the oxides of U and Pu, confirming the validity of the approach. An evaluation of state occupations supports the proposal that the occupation of the 5f levels in bulk Pu must be near 5.

Acknowledgements

Lawrence Livermore National Laboratory is operated by Lawrence Livermore National Security, LLC, for the U.S. Department of Energy, National Nuclear Security Administration under Contract No. DE-AC52- 07NA27344. JGT and SWY were supported by the DOE Office of Science, Office of Basic Energy Science, Division of Materials Science and Engineering. Work at the RAS and VNIITF was supported in part by Contract B590089 between LLNL and VNIITF. The Advanced Light Source (ALS) in Berkeley and the Stanford Synchrotron Radiation Laboratory are supported by the DOE Office of Science, Office of Basic Energy Science .

References

1. M. G. Mason, .S.-T. Lee, and G. Apai, H.. F. Davis, D. A. ShirleyA. Franciosi and J. H. Weaver, Phys. Rev. Lett. 47, 730 (1981); S.-T. Lee, G. Apai, M. G. Mason**,** R. Benbow and Z. Hurych, Phys. Rev. B 23, 505 (1981); M.G. Mason, Phys. Rev. B 27, 748 (1983).

2. J. G. Tobin, S. W. Robey, L. E. Klebanoff, and D. A. Shirley, Phys. Rev. B 28, 6169 (1983).

3. V. L. Colvin, A. P. Alivisatos, and J. G. Tobin, Phys. Rev. Lett. **66**, 2786 (1991).

4. J. G. Tobin, B. W. Chung, R. K. Schulze, J. Terry, J. D. Farr, D. K. Shuh, K. Heinzelman, E. Rotenberg, G. D. Waddill, and G. van der Laan, Phys. Rev. B **68**, 155109 (2003)

5. L. Havela, T. Gouder, F. Wastin, and J. Rebizant, Phys. Rev. B 65, 235118 (2002).

6. T.W. Trelenberg, S.C. Glade, J.G. Tobin and A.V. Hamza, Surface Science **600**, 2338 (2006).

7. T.W. Trelenberg, S.C. Glade, T.E. Felter, J.G. Tobin and A.V. Hamza, Rev. Sci. Instrum. **75**, 713 (2004).

8. P. van Kampen, Ch. Gerth, M. Martins, P. K. Carroll, J. Hirsch, E. T. Kennedy, O. Meighan, J.-P. Mosnier, P. Zimmermann, and J. T. Costello, Phys. Rev. A 61, 062706 (2000).

9. J. Han, V. Goncharov, L. A. Kaledin, Anatoly V. Komissarov and M. C. Heaven, J. Chem . Phys. 120, 5155 (2004)

10. J. Marcalo and J.K. Gibson, J. Phys. Chem. A 113, 12599 (2009).

11. L. Gagliardi, M. C. Heaven, J. Wisborg Krogh, and B. O. Roos, J. Amer. Chem. Soc. 127, 86 (2007).

12. Jun Li, B. E. Bursten, L. Andrews, and C. J. Marsden, J. Amer. Chem. Soc. 126, 3424 (2004).

13. I. D. Prodan, G. E. Scuseria, and R. L. Martin, Phys. Rev. B 76, 033101 (2007).

14. M.V. Ryzhkov and A.Ya. Kupryazhkin, J. Nucl. Materials 384, 226 (2009).

15. J.-P. Dognon, C. Clavague´ and P. Pyykko, J. Amer. Chem. Soc. 131, 238 (2009).

16. D. L. Clark, G. R. Choppin, C. S. Dayton, D. R. Janecky, L. J. Lane and I. Paton, J. Alloys Cmpds 444–445, 11 (2007).

17. S.D. Conradson, B. D. Begg, D. L. Clark, C. Den Auwer, F. J. Espinosa-Faller, P. L. Gordon, N. J. Hess,| R. Hess, D. W. Keogh, L. A. Morales, M.P. Neu, W. Runde, C. D. Tait, D. K. Veirs, and P. M. Villella, Inorg. Chem. 42, 3715 (2003).

18. D. L. Clark, D. E. Hobart, and M. P. Neu, Chem. Rev. 95, 25 (1995).

19. J.G. Tobin, P. Söderlind, A. Landa, K.T. Moore, A.J. Schwartz, B.W. Chung, M.A. Wall, J.M. Wills, R.G. Haire, and A.L. Kutepov, J. Phys. Cond. Matter **20**, 125204 (2008).

20. A. Mirmelstein and M. Ryzhkov, Reports on the results of Contract B590089; J. G. Tobin, M. Ryzhkov, A. Mirmelstein, "Contract B590089: Technical Evaluation of the Pu Cluster Calculations," LLNL-TR-516874, LLNL, Livermore, CA, USA, 2011.

21. A. Rosen A. and D.E. Ellis, J. Chem. Phys. 62, 3039 (1975).

22. M. V. Ryzhkov, N. I. Medvedeva and V. A. Gubanov, Physica Scripta 48, 629 (1993).

23. M.V. Ryzhkov et al., Radiochimica Acta, (1992).

24. B. Delley, J. Chem. Phys. 92, 508 (1990); B. Delley, J. Chem. Phys. 113, 7756 (2000).

25. J. Kubler and V. Eyert, Electronic Structure Calculations in Materials Science and Technology. Vol. 3A: Electronic and Magnetic Properties of Metals and Ceramics. Part I. Volume Ed.: K.H.J. Buschow (VCHVerlag, Weinheim, 1992), p. 1-145

26. S.-W. Yu, J. G. Tobin, P. Olalde-Velasco, W. L. Yang, and W. J. Siekhaus," J. Vac. Sci. Tech. A. 30, 011402 (2012).

27. J.G. Tobin and S.-W. Yu, Phys. Rev. Lett, **107,** 167406 (2011).

28. S.-W. Yu, J. G. Tobin, J. C. Crowhurst, S. Sharma, J. K. Dewhurst, P. Olalde-Velasco, W. L. Yang, and W. J. Siekhaus, Phys. Rev. B **83**, 165102 (2011).

29. S.-W. Yu, J. G. Tobin, and B. W. Chung, Rev. Sci. Instrum. **82**, 093903 (2011).

30. M.V. Ryzhkov, I.R. Shein, and A.L. Ivanovskii, "Electronic structure of actinide dimers," Phys. Rev A, submitted 2011.

31. O. Gunnarsson, B.I. Lundqvist, Phys. Rev.B. **13,** 4274 (1976).

32. M.V. Ryzhkov, N.I. Medvedeva, V.A. Gubanov, J. Phys. Chem. Solids **56,** 1231 (1995).

33. M.V. Ryzhkov, T.A. Denisova, V.G. Zubkov, L.G. Maksimova, J. Struct. Chem. **41,** 927 (2000).

34. D.E. Ellis, G.A. Benesh, E. Byrom, Phys. Rev.B. **20** (1979) 1198.

35. J. J. Yeh and I. Lindau, At. Data Nucl. Data Tables **32**, 1 (1985).

36. N. W. Ashcroft and N.D. Mermin, "Solid State Physics," Holt Rinehart and Winston, New York, 1976.

Tables

Table 1: Individual and average configurations of Pu atom in Pu_{19} and Pu_{79} clusters in δ-Pu

Cluster	Pu Site	Configuration
Pu_{19} cluster	Pu1 (one central atom)	$5f^{5.48}6d^{3.22}7s^{0.08}7p^{-0.54}$
(3 types of symmetrically	Pu2 (12 neighbors of central atom)	$5f^{5.55}6d^{1.96}7s^{0.43}7p^{0.23}$
non-equivalent sites)	Pu3 (6 next neighbors of central atom)	$5f^{5.91}6d^{0.97}7s^{0.59}7p^{0.16}$
	Average configuration*	**$5f^{5.66}6d^{1.71}7s^{0.46}7p^{0.17}$**
	(*Total number of valence electrons is 8.0)	
Pu_{79} cluster	Pu1 (one central atom)	$5f^{5.51}6d^{2.67}7s^{0.30}7p^{-0.23}$
(6 types of symmetrically	Pu2 (12 neighbors of central atom)	$5f^{5.51}6d^{2.85}7s^{0.22}7p^{-0.27}$
non-equivalent sites)	Pu3 (6 next neighbors of central atom)	$5f^{5.48}6d^{2.96}7s^{0.19}7p^{-0.12}$
	Pu4 (24 atoms of the next coord. sphere)	$5f^{5.90}6d^{2.50}7s^{0.41}7p^{0.17}$
	Pu5 (12 atoms of the next coord. sphere)	$5f^{5.14}6d^{1.87}7s^{0.47}7p^{0.31}$
	Pu6 (24 atoms of the next coord. sphere)	$5f^{4.72}6d^{1.40}7s^{0.45}7p^{0.28}$
	Average configuration*	**$5f^{5.33}6d^{2.16}7s^{0.38}7p^{0.13}$**
	(*Total number of valence electrons is 8.0)	

Table 2

Pu Dimer	$5f^{5.85}6d^{0.58}7s^{1.40}7p^{0.17}$	Ref. 20, 30
Pu Atom	$5f^{6}6d^{0}7s^{2}$	Ref. 36

Figure Captions

Figure 1 The structures of δ-Pu-like Pu_{19} and Pu_{79} clusters are shown here. The Pu_{79} cluster contains a Pu_{19} cluster as a "core" (showed as the dark spheres). Pu1 is the central atom of the Pu_{19} cluster: twelve Pu2 and six Pu3 atoms form its nearest neighbors and the next nearest neighbors, respectively.

Figure 2 A comparison of the Density of States (DOS) for the central part of a $U_{63}O_{216}$ cluster [14] with spectroscopic results from a bulk UO_2 sample. [26-28] The Occupied Density of States (ODOS) is compared to the data from X-ray Photoelectron Spectroscopy (XPS). The Unoccupied Density of States (UDOS) is compared to the X-ray Absorption Spectroscopy (XAS) and Bremstrahlung Isochromat Spectroscopy (BIS) data. Partial and total DOS are provided. The spectroscopic data are representative of experimental DOS estimates, although skewed by cross-sectional effects. [26-28]

Figure 3 A comparison of the Density of States (DOS) for the central part of a $Pu_{63}O_{216}$ cluster [14] with spectroscopic results from a slightly oxidized bulk Pu sample. [4, 19] The Occupied Density of States (ODOS) is compared to the data from synchrotron-radiation-based Photoelectron Spectroscopy (PES). Partial and total DOS are provided. The spectroscopic data are representative of experimental DOS estimates, although skewed by cross-sectional effects. By working at

the Cooper Minimum, the non-5f features are emphasized. Please see the text for detail.

Figure 4 Total and partial densities of states for the central atom Pu1 of a Pu_{19} cluster.

Figure 5 Total and partial densities of states for the central Pu1 atom in a Pu_{79} clusters.

Figure 6 Total and partial density of states for the nearest neighboring Pu_2 sites in Pu_{79} cluster.

Figure 7 Spectroscopic results from a slightly oxidized bulk Pu sample are shown here. [4, 19] The Occupied Density of States (ODOS) in Figures 4-6 can be compared to the data from synchrotron-radiation-based Photoelectron Spectroscopy (PES). The spectroscopic data are representative of experimental DOS estimates, although skewed by cross-sectional effects. By working at the Cooper Minimum at hv = 225 eV, the non-5f features are emphasized. The Pu 5f is most strongly emphasized on resonance at hv = 125 eV. At the anti-resonance, hv = 100 eV, the Pu 6d is part of the remnant intensity at the Fermi Edge. (Binding energy = 0 eV) Please see the text for detail.

Figure 8 Plot of PU 5f occupation from Tables 1 and 2 versus the cube root of the number of Pu atoms. ($\sqrt[3]{N}$) For an atom with N = 1, $\sqrt[3]{N} = 1$; For a dimer with N = 2, $\sqrt[3]{N} = 1.26$; For Pu_{19} cluster with N = 19, $\sqrt[3]{N} = 2.67$; For a Pu_{79} cluster with N = 79, $\sqrt[3]{N} = 4.2$. Also shown is the least squares fitted line and the extrapolation to N = 125, $\sqrt[3]{N} = 5$, N = 216,

$^3\sqrt{N} = 6$ and N = 343, $^3\sqrt{N} = 7$, as well as the result from the bulk Pu spectroscopic studies. [19]

Figure 9 X-ray absorption spectroscopy results for the 4d and 5d levels of plutonium and uranium. The Uranium spectrum in the lower panel is from the Stanford Synchrotron Radiation Laboratory. [19] All other spectroscopic results in this article are from the Advanced Light Source in Berkeley. [4,19, 26] See text for details.

Figures

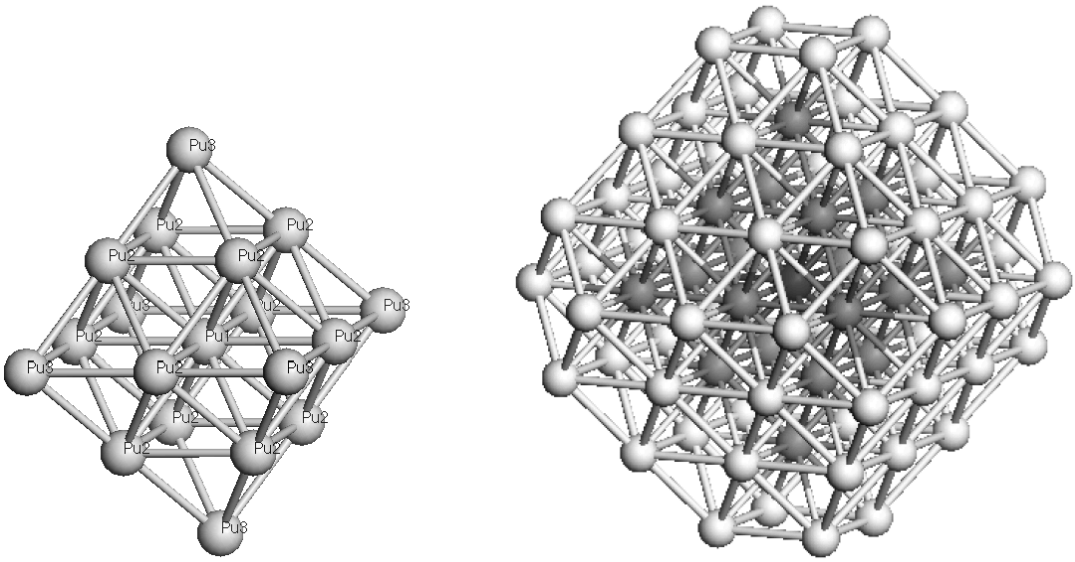

Figure 1

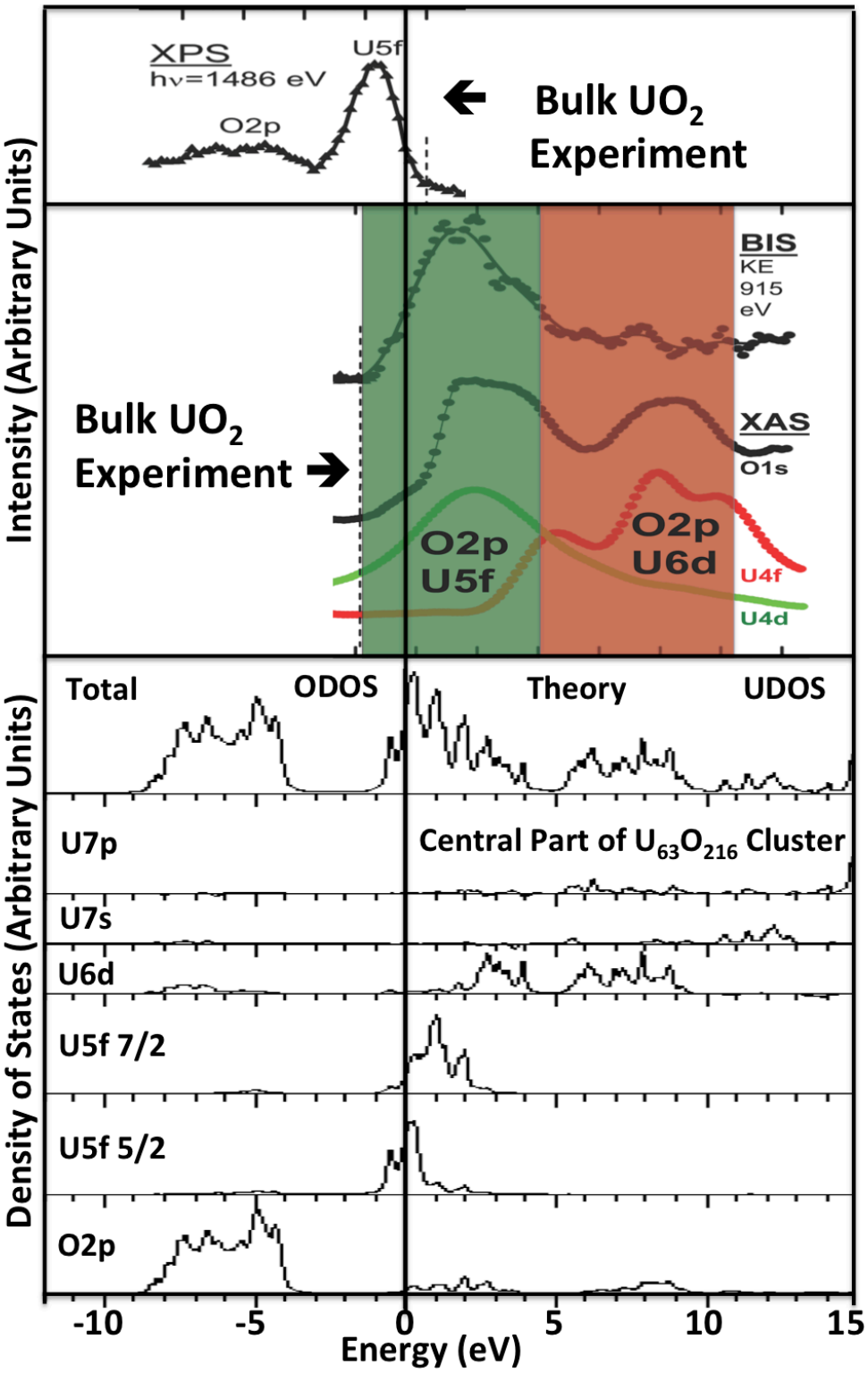
XPS
hν=1486 eV
U5f
O2p
Bulk UO2
Experiment
BIS
KE
915
eV
XAS
O1s
Bulk UO2
Experiment
O2p
U5f
O2p
U6d
U4f
U4d
Intensity (Arbitrary Units)
Total
ODOS
Theory
UDOS
U7p
Central Part of U63O216 Cluster
U7s
U6d
U5f 7/2
U5f 5/2
O2p
Density of States (Arbitrary Units)
-10
-5
0
5
10
15
Energy (eV)

Figure 2

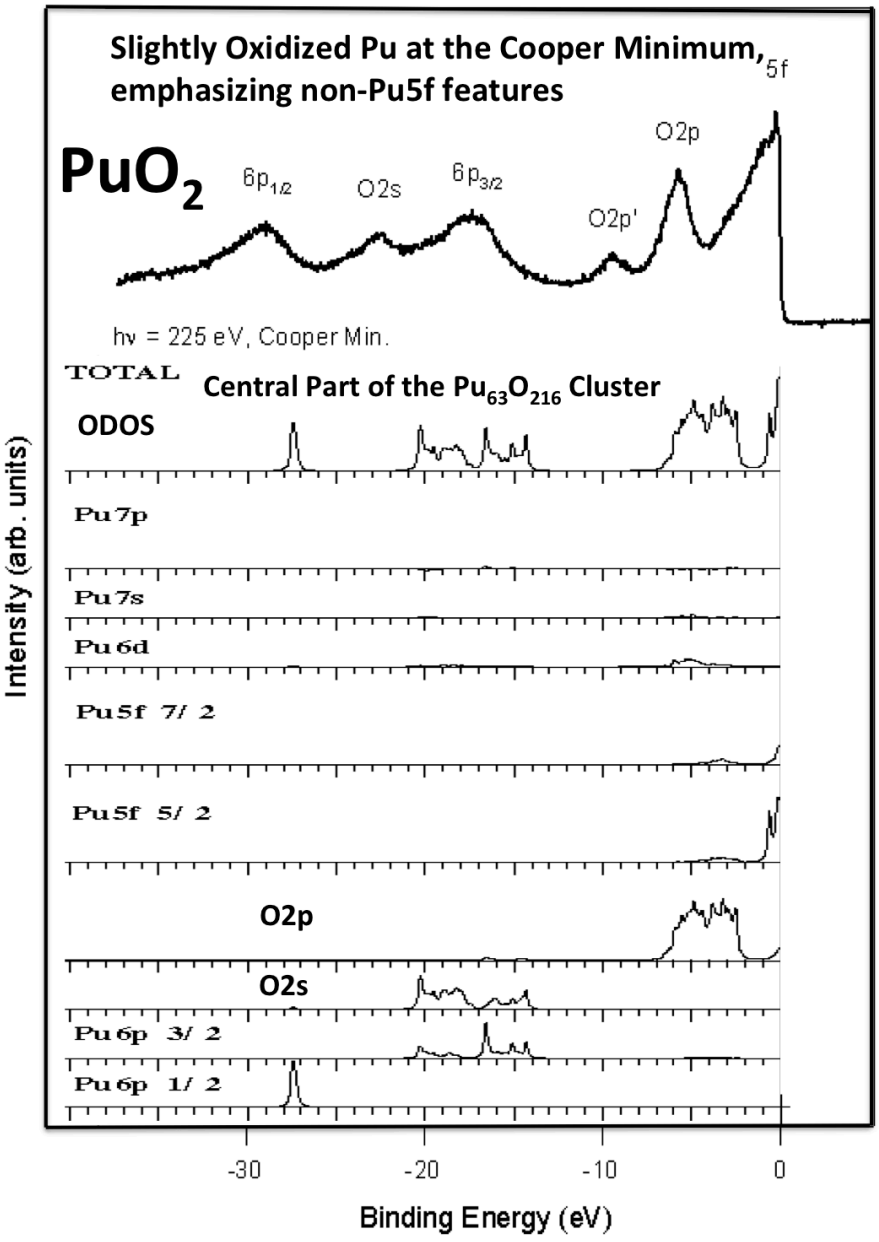
Slightly Oxidized Pu at the Cooper Minimum, emphasizing non-Pu5f features
5f
PuO2
6p1/2
O2s
6p3/2
O2p'
O2p
hν = 225 eV, Cooper Min.
TOTAL
Central Part of the Pu63O216 Cluster
ODOS
Pu 7p
Pu 7s
Pu 6d
Pu 5f 7/ 2
Pu 5f 5/ 2
O2p
O2s
Pu 6p 3/ 2
Pu 6p 1/ 2
Intensity (arb. units)
-30
-20
-10
0
Binding Energy (eV)

Figure 3

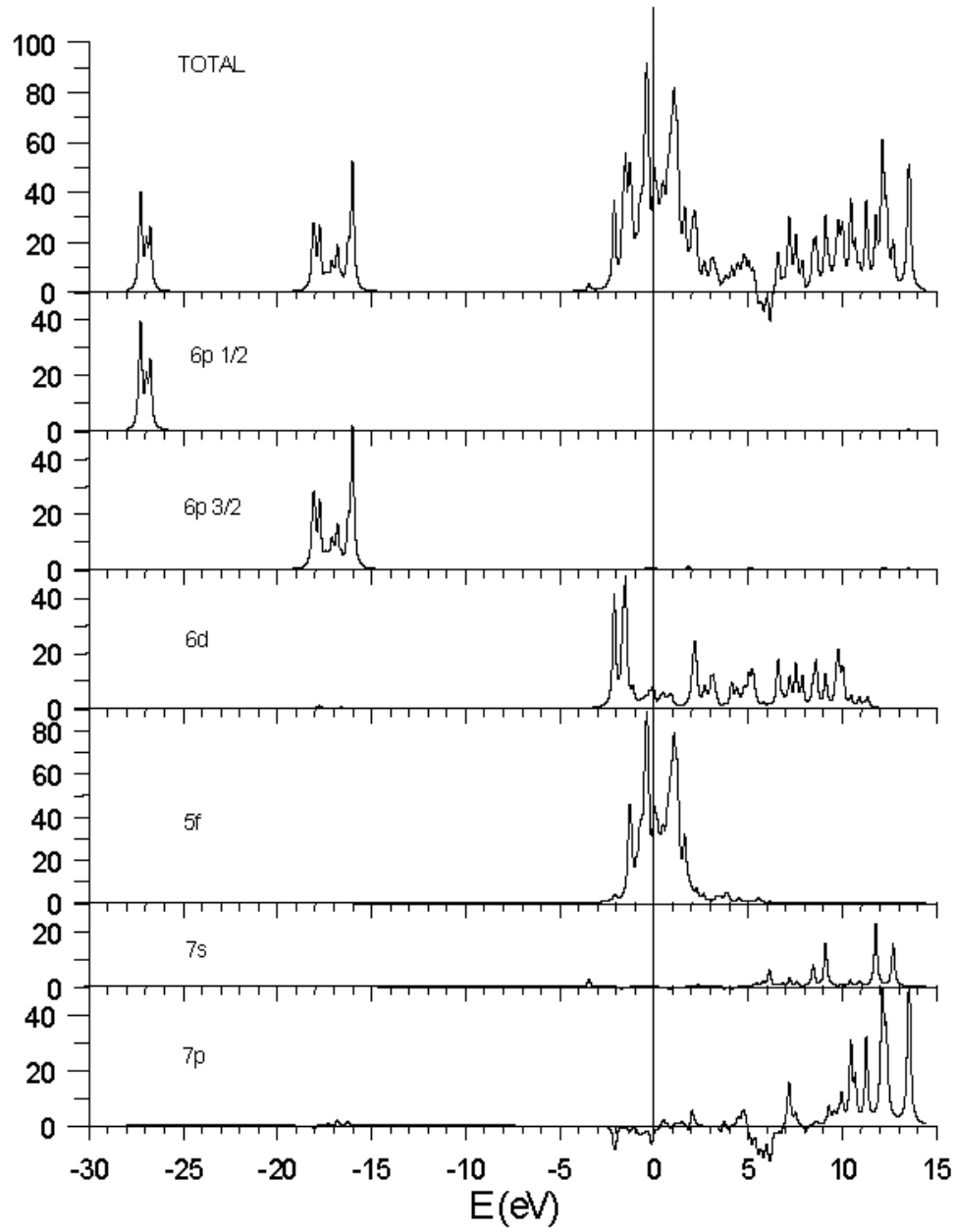

Total and partial densities of states for the Pu_{19} cluster.

Figure 4

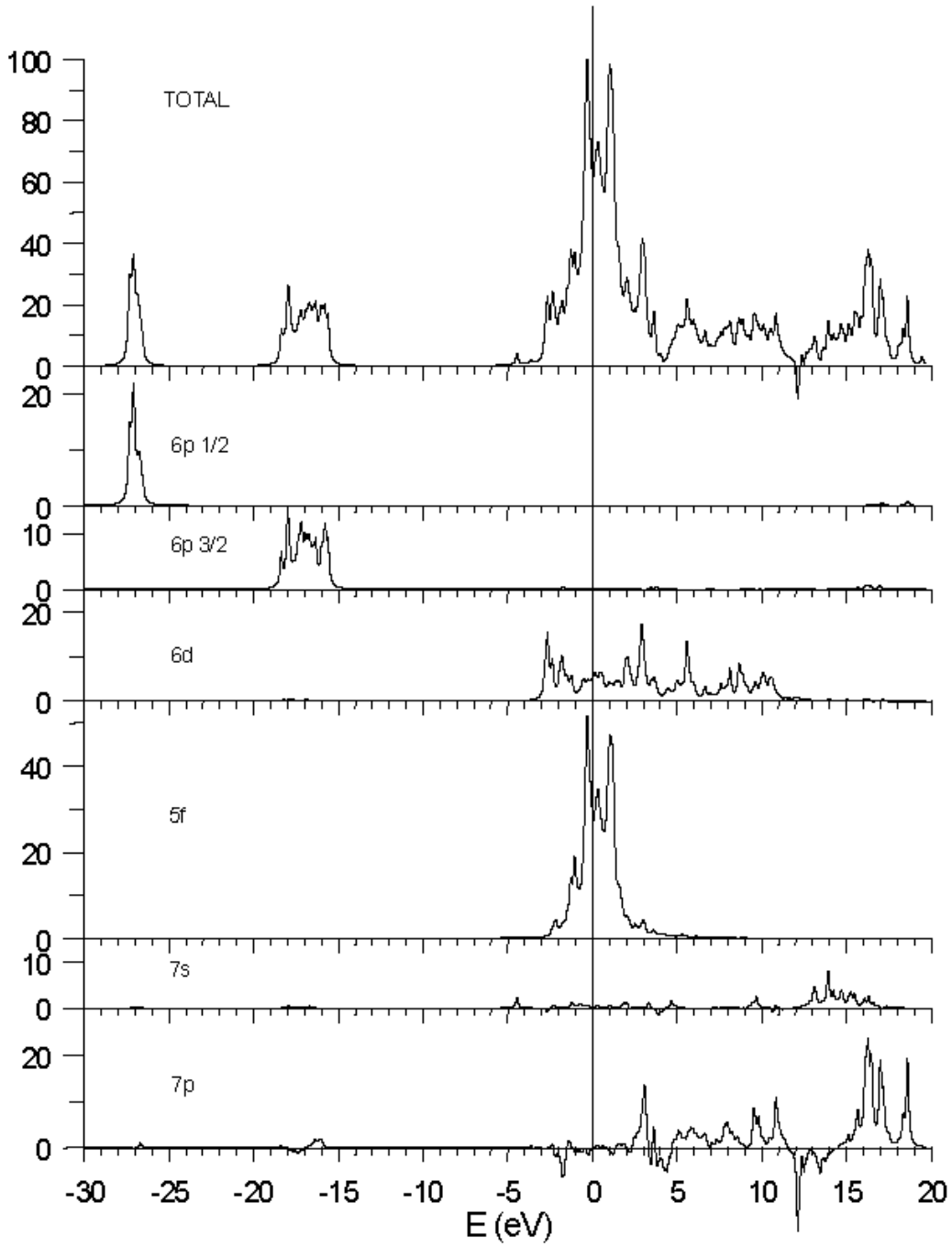

Pu_{79}

Figure 5

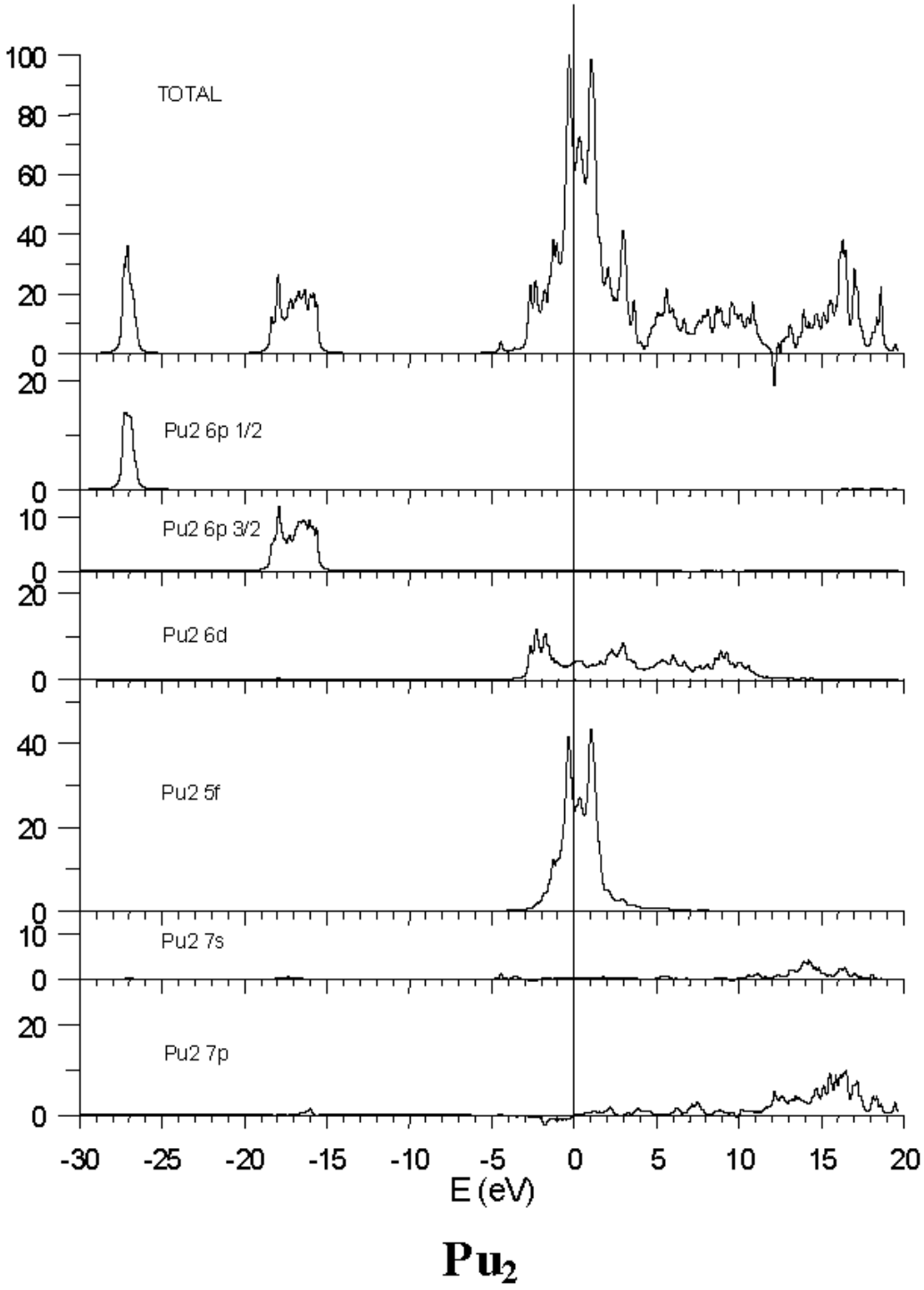

Figure 6

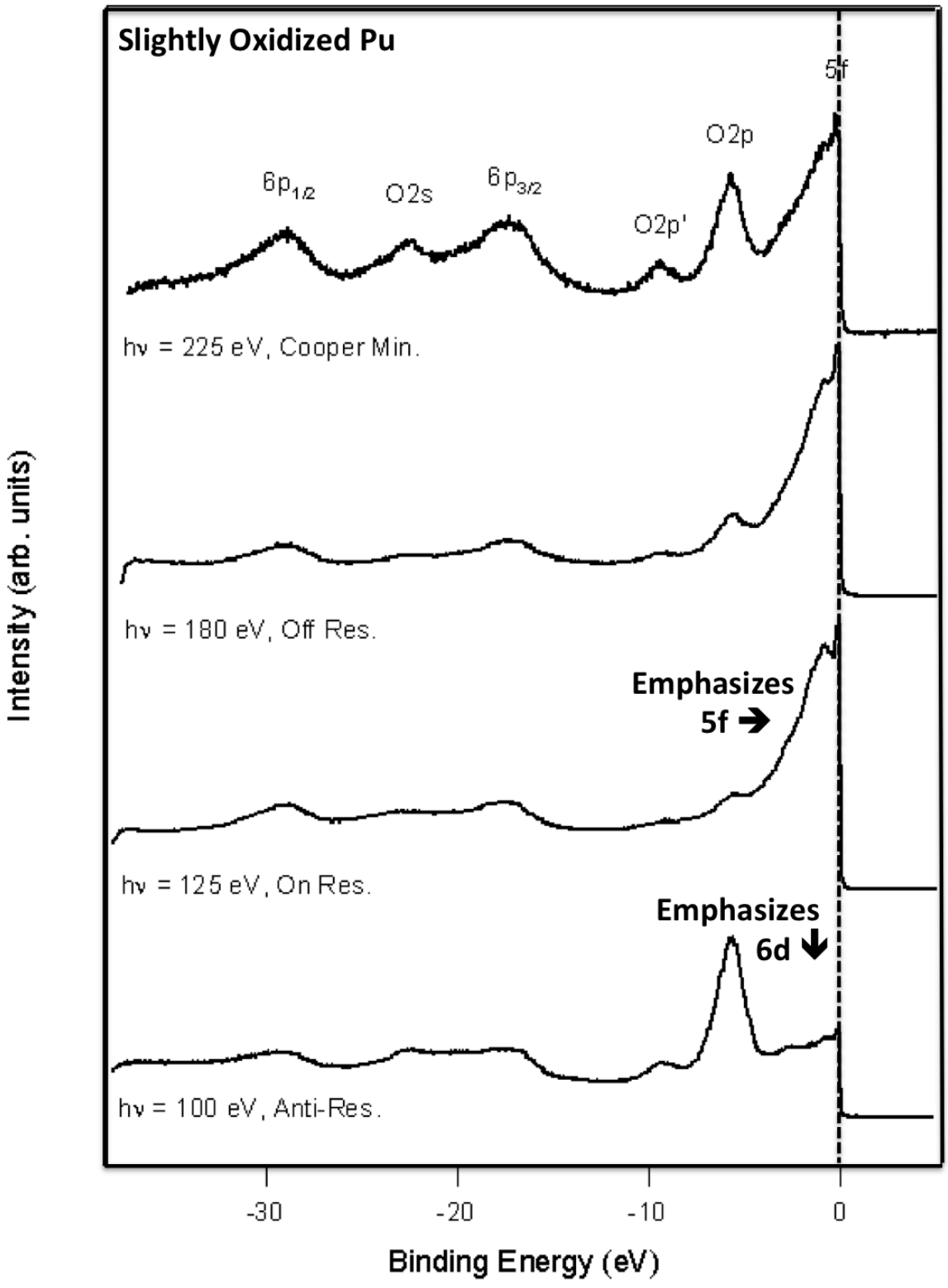
Slightly Oxidized Pu
5f
O2p
6p1/2
O2s
6p3/2
O2p'
hν = 225 eV, Cooper Min.
hν = 180 eV, Off Res.
Emphasizes
5f
hν = 125 eV, On Res.
Emphasizes
6d
hν = 100 eV, Anti-Res.
Intensity (arb. units)
-30
-20
-10
0
Binding Energy (eV)

Figure 7

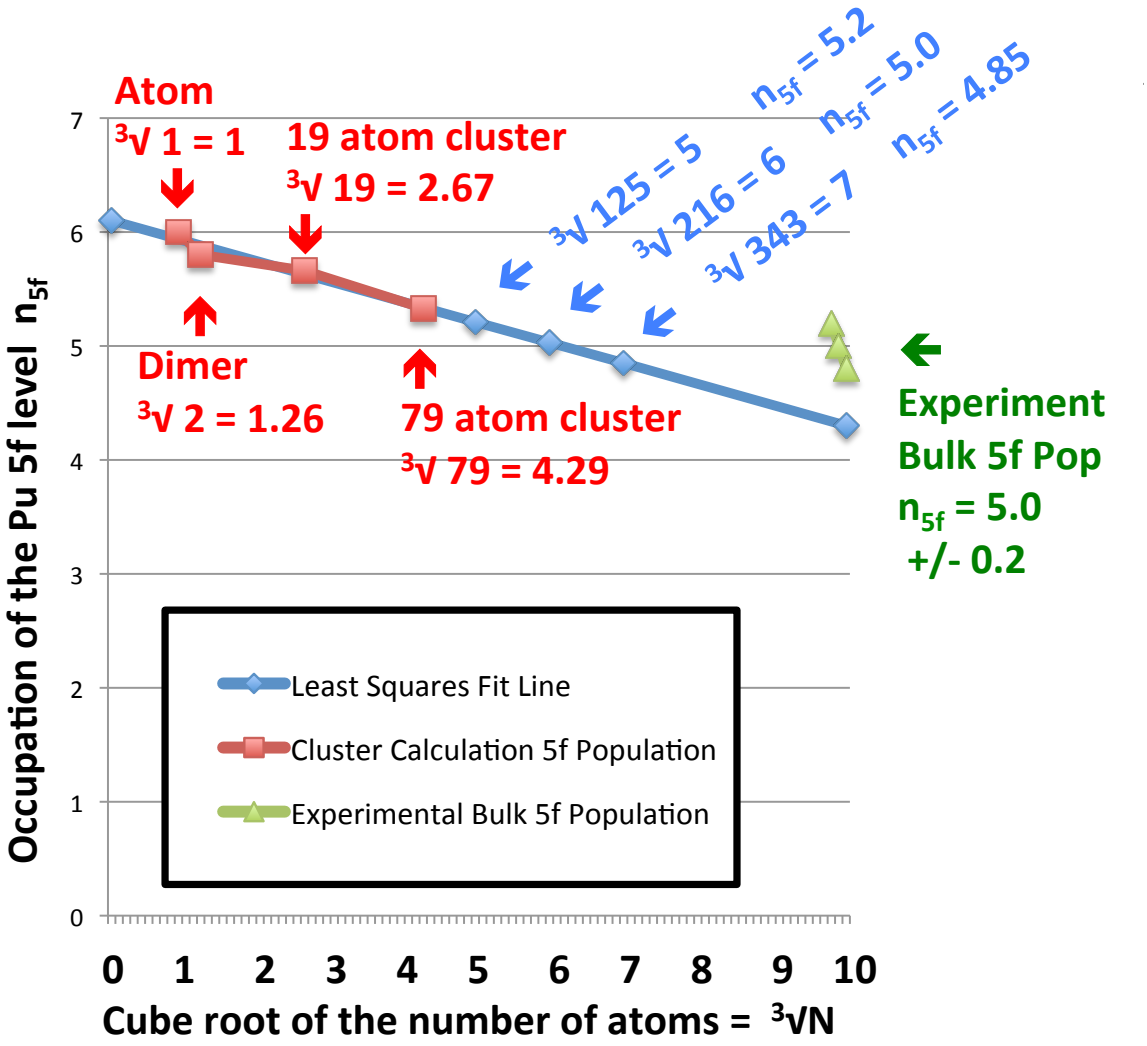
Atom
$^3\sqrt{}$ 1 = 1
19 atom cluster
$^3\sqrt{}$ 19 = 2.67
$^3\sqrt{}$ 125 = 5
$^3\sqrt{}$ 216 = 6
$^3\sqrt{}$ 343 = 7
n_{5f} = 5.2
n_{5f} = 5.0
n_{5f} = 4.85
Dimer
$^3\sqrt{}$ 2 = 1.26
79 atom cluster
$^3\sqrt{}$ 79 = 4.29
Experiment
Bulk 5f Pop
n_{5f} = 5.0
+/- 0.2
Least Squares Fit Line
Cluster Calculation 5f Population
Experimental Bulk 5f Population
Occupation of the Pu 5f level n_{5f}
0 1 2 3 4 5 6 7
0 1 2 3 4 5 6 7 8 9 10
Cube root of the number of atoms = $^3\sqrt{N}$

Figure 8

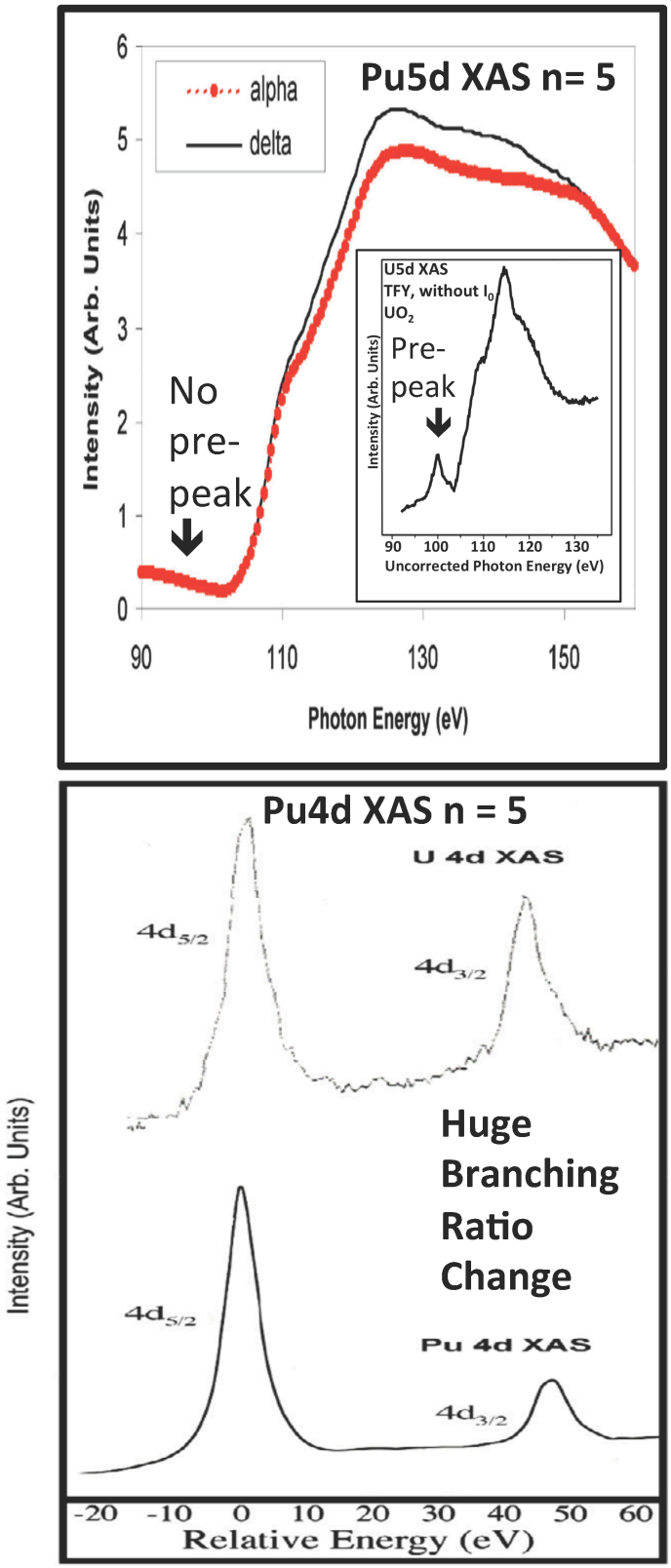
Pu5d XAS n= 5
alpha
delta
Intensity (Arb. Units)
No pre-peak
U5d XAS
TFY, without I_0
UO_2
Pre-peak
Intensity (Arb. Units)
90 100 110 120 130
Uncorrected Photon Energy (eV)
0 1 2 3 4 5 6
90 110 130 150
Photon Energy (eV)
Pu4d XAS n = 5
U 4d XAS
$4d_{5/2}$
$4d_{3/2}$
Huge Branching Ratio Change
$4d_{5/2}$
Pu 4d XAS
$4d_{3/2}$
Intensity (Arb. Units)
-20 -10 0 10 20 30 40 50 60
Relative Energy (eV)

Figure 9